CONTROL OF WAKE BEHIND A CIRCULAR CYLINDER USING RIBLET SURFACES

S. J. Lee
Department of Mechanical Engineering
Pohang University of Science and Technology, Pohang, 790-784, Korea
sjlee@postech.ac.kr

H. C. Lim
Department of Environmental Science and Engineering
Pohang University of Science and Technology, Pohang, 790-784, Korea
hclim@postech.ac.kr

ABSTRACT

Flow around circular cylinders with different groove surfaces (U and V-shaped) was investigated experimentally. The results were compared with those from a smooth cylinder of the same diameter D. The drag force, mean velocity and turbulence intensity profiles of the wake behind the cylinders were measured for Reynolds numbers in the range Re_D=8×10^3~1.4×10^5. At Re_D=1.4×10^5, the U-type groove surface reduced the drag coefficient by 18.6% compared with the smooth cylinder, whereas the drag reduction of V-type groove was only 2.5%. The two riblet surfaces tested in this study display different surface pressure distributions at high Reynolds numbers due to their different flow structures near the cylinder surface. Flow around the cylinders was visualized using a particle tracer technique to qualitatively investigate the flow structure. The longitudinal secondary vortices formed behind the grooved cylinders are more active and show rapid flow motion, compared with the smooth cylinder.

INTRODUCTION

Since the global "energy crisis" of the 1970s, drag reduction has received a great deal of attention in a variety of engineering applications. Recent advanced technologies, such as microfabrication and active feedback control, make it possible to employ artificial manipulations on drag force and acoustic noise. Since drag reduction is closely related with energy saving, extensive effort has been made over recent decades to reduce the drag acting on moving vehicles.

In order to reduce the drag force acting on a bluff body, it is necessary to accurately predict and effectively control the flow around the body. We can reduce the drag acting on the surface by changing the near-wall flow structure, especially by controlling the coherence structure (Cantwell, 1981 ; Robinson, 1991). Although flow control for drag reduction is very important in engineering applications and has attracted much academic interest, there are still many areas to be investigated.

Previous studies have revealed that the riblet surface with longitudinal grooves is an effective flow control technique for drag reduction and heat transfer enhancement. However, performance depends largely on the configuration of the groove surfaces.

Walsh (1983) investigated drag reduction of a flat surface with longitudinal ribs of rectangular, triangular, and transversely curved shapes. She found that the drag reduction was associated with a decrease of momentum thickness and turbulent velocity fluctuations, and depended mainly on the configuration of the ribs as determined by parameters such as the height (h), spacing (s), and shape. She obtained a maximum of 8% drag reduction for a symmetric V-groove surface of depth $h^+(= hu_\tau/\nu)$<25 and spacing $s^+(= su_\tau/\nu)$<200. Robert (1992) reported that a riblet surface attached on a practical air-plane reduced the drag coefficient by approximately 2% in real navigation tests.

Most previous studies on riblet surfaces have focused on the turbulent boundary layer over a flat surface. In applications of riblet surfaces on bluff bodies, Achenbach (1971) and Guven et al. (1980) found that the surface roughness on a circular cylinder affected the vortex shedding, the drag coefficient and heat-transfer characteristics. Ko et al. (1986) [xxx see note on this reference below] and Leung et al. (1991) measured the mean pressure distributions and Strouhal number variation for V-groove circular cylinders in the Reynolds number range 2×10^4~1.6×10^5. In their study, the V-groove and smooth cylinders had almost the same drag coefficient. They focused on the effect of different V-groove configurations on the drag reduction of a riblet cylinder.

Many previous studies have investigated the flow structure over simple riblet shapes such as a V-shaped groove. However, Walsh (1983) suggests that the semi-circular riblet with sharp peaks is one of the optimum riblet shapes for drag reduction. In addition, there are still some contradictions about the mechanism by which riblets reduce the drag acting on bluff bodies with riblet surfaces. In this study, the effect of the groove configuration (U and V-shaped) on a circular cylinder on the flow structure of the

near-wake and drag reduction has been investigated experimentally.

EXPERIMENTAL APPARATUS AND METHOD

Experimental apparatus and method

Experiments were performed in a closed-return type subsonic wind tunnel with a test section of 0.72 m width, 0.6 m height and 6 m length. The free stream turbulence intensity in the test section was less than 0.08% at U_0=10 m/s. This level of free stream turbulence is sufficient for the proposed study on the wake structure behind bluff bodies (Gerrard, 1954). The flow characteristics around the cylinders were measured with varying the Reynolds number (based on the cylinder diameter D) in the range Re_D=8,000~140,000.

Three circular cylinders of the same outer diameter (D=60mm) with different surface configurations were tested in this study. One cylinder had a smooth surface. The other two cylinders had longitudinal grooves, one with a saw-tooth (V-groove) shape, the other cylinder with a semi-circle (U-groove) shape. The experimental models were made of Teflon pipe of length 600 mm. The U-groove and V-groove cylinders have the same riblet spacing of s=3mm. However, the depth (h) of the U-grooves is half that of the V-grooves.

The cylinder models were installed horizontally 260 mm above the bottom surface of the wind-tunnel test section. A schematic diagram of the experimental set-up is given in Fig.1. Two square end-plates, 300 mm × 300 mm with a 2 mm thickness, were used to minimize the effect of a boundary layer developing along the tunnel sidewalls and to maintain two-dimensional flow characteristics in the cylinder wake. The shape and size of the plates were determined following the results of Stansby (1974).

Flow measurements

The wake behind a circular cylinder has organized coherent structure due to regular vortex shedding. These coherent structures are closely related to the generation and dissipation of turbulence energy and play an important role in drag reduction. Therefore, the flow characteristics of this coherent structure should be clarified to effectively control the aerodynamic drag force.

Wake velocity profiles were measured using I-type (DANTEC 55P11) and X-type hot-wire probes (Dantec 55P61) connected to a constant temperature hot-wire anemometer (TSI IFA 100) and DT2838 A/D converter. The hot-wire probe was traversed to the measuring positions using a 3-D traverse system with an accuracy of 0.01 mm. At each measurement point, 32768 velocity data were acquired at 2000 samples/sec after low-pass filtering at 800 Hz. During the experiments, the temperature variation in the wind tunnel test-section was maintained to be

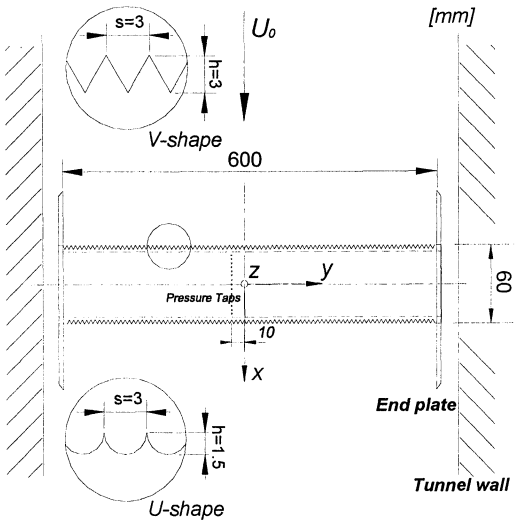

Fig.1 Wind tunnel test section and experimental setup

less than 0.5 °C. The vertical mean velocity and turbulence intensity profiles were measured in the range z/D= –3~3 at 0.1D intervals at the downstream sections of x/D= 4 and 6. To investigate the vortex structure of the near wake behind the cylinder, the dominant shedding frequency of velocity signals from an I-type hot-wire probe located at x/D=2, y/D=0.5 was spectrally analyzed.

Aerodynamic forces acting on the cylinders were measured using a 3-component load-cell (Nissho LMC-3502) with high sensitivity and linearity. The load-cell was coupled to a high-gain DC strain amplifier (DSA-100), and connected to a personal computer through a DT2838 A/D converter.

For low-speed incompressible flow past bluff bodies, the drag coefficient is a function only of the Reynolds number based upon the free-stream U_0 and cylinder diameter D.

The drag coefficient based on the effective frontal area of the cylinder A is as follows:

$$C_D = \frac{2 \times Drag}{\rho U_0^2 A} \qquad (1)$$

In general, the drag force acting on a bluff body is composed of pressure drag and friction drag. For a circular cylinder, the pressure drag is dominant.

To measure surface pressure distributions, 36 taps were installed along the longitudinal axis of the cylinder at a 10 mm interval from the midsection of the wind tunnel. Pressure distributions were measured by rotating the cylinder in 10-degree increments. The inner diameter of the stainless steel pressure taps was 0.8 mm. The pressure taps were connected to a micromanometer (FCO-19), and the analog pressure signals were digitized using a high-precision A/D converter (DT-2838). At each measurement point, 16384 pressure data were acquired at a 500 Hz sampling rate after low-pass filtering at 200 Hz. A time delay of a few seconds

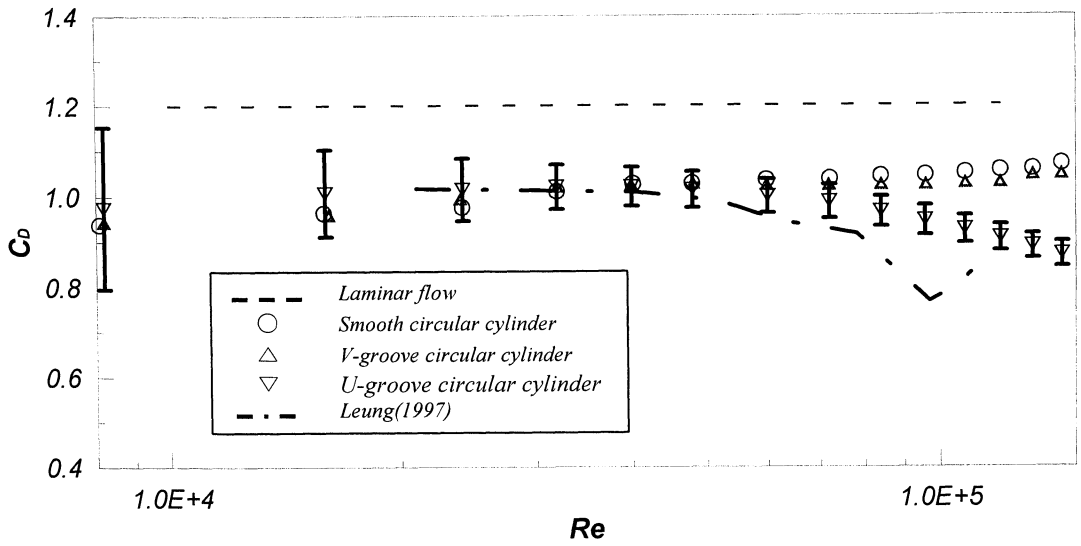

Fig.2 Variation of drag coefficient with Reynolds number

was given to recover pressure fluctuations after each channel scanning.

The particle tracer technique was employed to visualize the flow pattern in the wake behind the cylinder. Poly-vinyl-chloride particles with an average diameter of 300 μm were seeded as tracer particles in a circulating water channel with a test section of $0.3W \times 0.25H \times 1.2L$ (m^3). The particle path-lines were illuminated with a thin cold light-sheet, emitted from a 150 W halogen lamp. The scattered particle images at a free stream velocity of 20 cm/s (Re=12,500) were photographed with a Nikon F5 camera.

RESULTS AND DISCUSSION

Drag force

Fig.2 shows the variation in drag coefficient with varying Reynolds number. The dotted line represents the conventional drag coefficient of a 2-D circular cylinder at Re ≥ 10^4. For comparison, the result of Ko et al. (1986) is included, marked as a dash-dot line. Although the general trend is similar, Ko's result has smaller C_D values at high Reynolds numbers. This may result from the difference between our riblet geometry and experimental conditions and those used by Ko.

Error bars indicate the error encountered in obtaining the mean values; the confidence level is 95%. The error shows large deviations at low Reynolds numbers due to the high sensitivity of the load-cell installed. As the Reynolds number increases, however, the error gradually decreases.

The drag coefficient of the cylinder models used in this study is lower than that of a general 2-D cylinder. This seems to be caused by 3-dimensional flow effects due to the relatively small aspect ratio of the cylinders used (L/D=10). For the smooth cylinder, the drag coefficient gradually increases with increasing Reynolds number. The drag

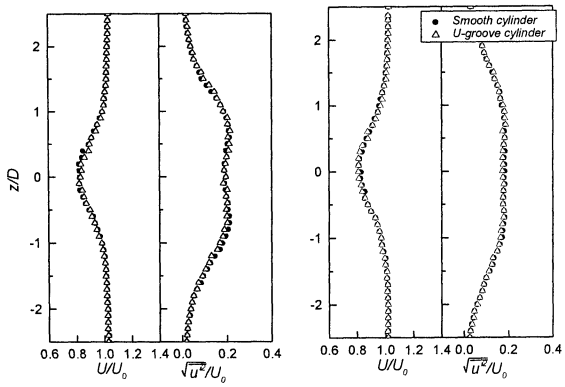

(a) x/D=4 (b) x/D=6

Fig.3 Streamwise mean velocity and turbulence intensity profiles at U_0=10m/s

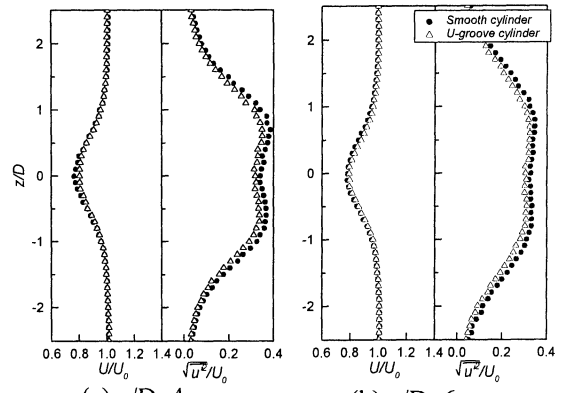

(a) x/D=4 (b) x/D=6

Fig.4 Streamwise mean velocity and turbulence intensity profiles at U_0=20m/s

coefficients of the smooth cylinder are in good agreement with previous results within the subcritical regime regime (Achenbach, 1971 ; Guven et al., 1980).

The drag coefficients of the riblet cylinders show a similar tendency to the smooth cylinder up to a

Reynolds number of 4×10^4. Thereafter, the drag coefficient of the cylinder with U-grooves decreased substantially. Ko et al. (1986) found similar behavior for a V-groove cylinder in the Reynolds number range from 2×10^4 to 1.6×10^5. He mentioned that the transitions from subcritical to critical and from critical to supercritical flow regimes for the V-groove cylinder occur at lower Reynolds numbers than for the smooth cylinder. In our study, the flow regime does not reach the critical Reynolds number; however, the drag coefficients of the smooth and V-groove cylinders show similar trends with respect to Reynolds number.

The V-groove cylinder shows drag reduction of about 2.5%, compared with that of the smooth circular cylinder in the subcritical regime. The drag coefficient of the U-groove circular cylinder, however, is reduced by 18.6% at $Re_D = 1.4\times10^5$.

Flow characteristics

Figs.3 and 4 show vertical profiles of the streamwise mean velocity and turbulence intensity measured at downstream locations of x/D=4 and 6 for two Reynolds numbers, $Re_D=4\times10^4$ (U_0=10m/s) and 8×10^4 (U_0=20m/s). The mean streamwise velocity profiles show a velocity deficit in the wake region behind the cylinder. Furthermore, the turbulence intensity profiles have double peaks. The turbulent kinetic energy has a tendency to propagate the velocity fluctuations in the near wake to the outer layer and dissipate the large-scale vortex structure into small-scale eddies. The wake width at x/D=6 is a little wider than that at x/D=4. The mean velocity and turbulence intensity of the streamwise velocity measured at x/D=4 and 6 show little difference between the smooth cylinder and the U-groove cylinder.

Fig. 4 shows the streamwise mean velocity and turbulence intensity profiles at U_0=20m/s ($Re_D = 8\times10^4$). As the Reynolds number increases, the flow structure shows a slightly larger difference between the smooth and U-groove cylinders, compared with that at U_0=10m/s. In addition, the turbulence intensity profiles have more distinct double-peaks and larger values than those at U_0=10m/s. From the smaller velocity deficit observed and momentum conservation theorem, it can be conjectured that the U-groove cylinder causes less drag than the smooth cylinder.

The U-groove cylinder has a higher mean velocity and lower turbulent fluctuations in the near wake in comparison with the smooth cylinder. This seems to be caused by the riblet surface reducing viscous damping and velocity fluctuations. From this, we can see that the total drag of the U-groove cylinder is smaller than that of the smooth cylinder.

Surface pressure distribution

The pressure distributions measured on the cylinder surface are shown in Fig.5. For the smooth circular cylinder, the surface pressure distribution does not show remarkable variation as the Reynolds number increases. This can be attributed to the fact that the flows tested are still within the subcritical Reynolds number regime (Bearman, 1969). For the V-groove cylinder (Fig.5(b)), the mean pressures on the cylinder surface after laminar separation are nearly constant, except for the high Reynolds number of Re_D=132,000.

The pressure distributions of the U-groove cylinder (Fig.5(c)) are quite different from those of the smooth and V-groove cylinders, even though the flow is within the subcritical regime. The surface pressure distribution has large variations around the separation region over the cylinder. As the Reynolds number increases, the separation point shifts downstream and the surface pressure decreases. This may be attributed to the fact that the riblet grooves

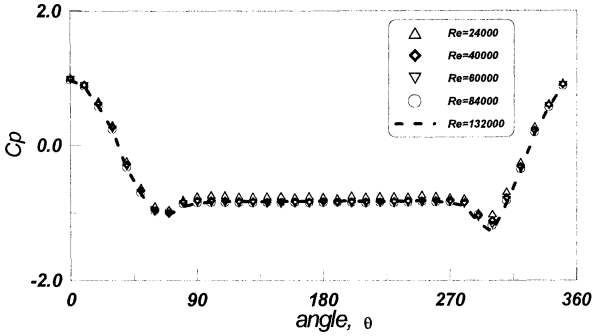

(a) Smooth circular cylinder

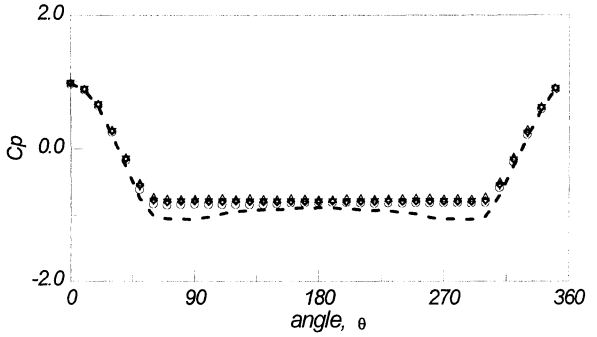

(b) V-groove circular cylinder

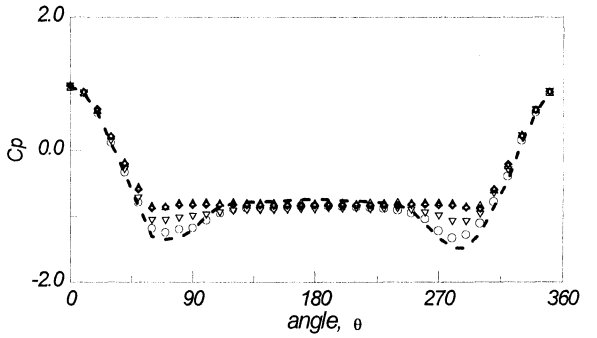

(c) U-groove circular cylinder

Fig.5 Comparison of surface pressure distributions

on the cylinder surface enhance the boundary layer transition from laminar to turbulent flow. In addition, the base pressure at Reynolds number Re_D=1.32×10^5 is higher than that at Reynolds number Re_D= 2.4×10^4. From these results, it can be conjectured that the U-groove surface causes a substantial decrease in the drag at high Reynolds numbers, compared with the other two cylinders.

Spectral analysis

Power spectral density (PSD) distributions measured at location x/d=2, y/d=0.5 are shown in Fig.6 for four Reynolds numbers: Re_D=24,000, 40,000, 56,000 and 96,000. For the smooth cylinder, the peak frequency and PSD value at this peak increase as the Reynolds number increases. Here, clear and distinct peak indicates the existence of a large vortical structure due to regular vortex shedding.

The U-groove cylinder has similar PSD distributions. However, the peak frequency is larger than that of the smooth cylinder at the same Reynolds numbers. These results have a correspondence with the results of vortex formation region.

Flow visualization

In present study, the flow structure was visualized using the particle tracer method. Fig.7 shows the particle streaks in the horizontal plane of the wake for the smooth, V-groove and U-groove cylinders at Reynolds number Re_D= 12,500.

These figures show longitudinal secondary vortices formed behind the cylinders. The flow past the smooth circular cylinder has nearly straight pathlines, compared with the flow around the U-groove cylinder. However, the longitudinal vortices formed behind the grooved cylinders are more active and show more rapid motion than those of the smooth cylinder. In addition, the secondary vortices formed behind the U-groove cylinder are located much closer to the cylinder, compared with the other two cases.

From these results we can see that the grooved surface changes the flow structure near the cylinder, causing a boundary transition and controlling the vortical structure in the near-wake.

From this, we can see that the groove surface changes the flow structure near the cylinder, causing boundary transition and controlling vortical structure

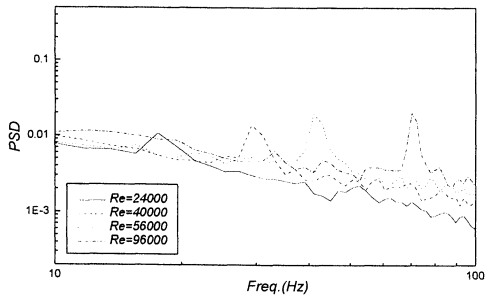

(a) Smooth cylinder

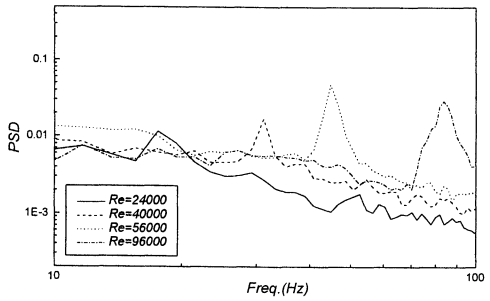

(b) U-grooved cylinder

Fig.6 Comparison of power spectral density distribution

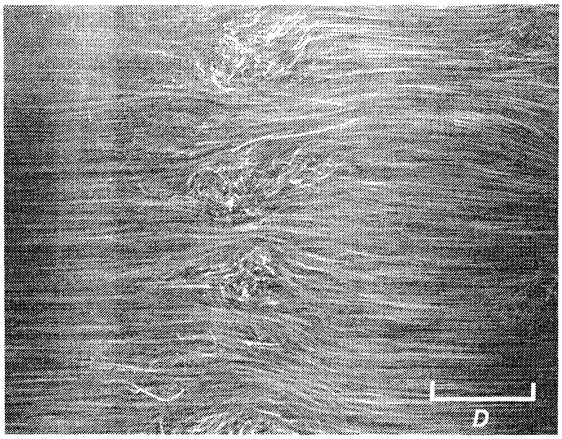

(a) Smooth circular cylinder

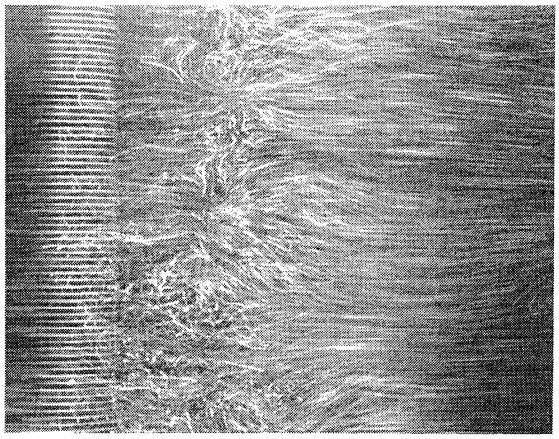

(b) V-groove cylinder

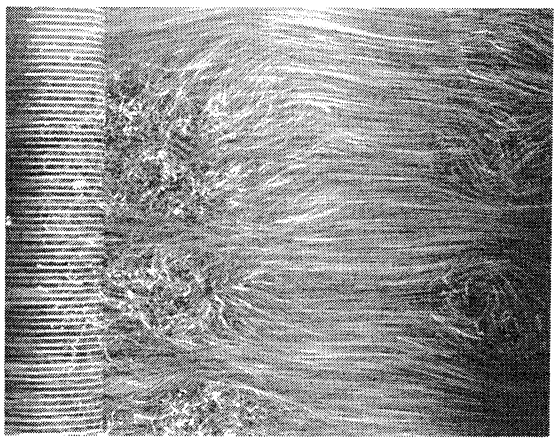

(c) U-groove cylinder

Fig.7 Flow visualization in horizontal plane

in the near-wake.

CONCLUSION

The flow characteristics of the wake behind circular cylinders with different groove configurations (U and V-shape) have been investigated experimentally. The drag force, wake velocity and surface pressure distribution were measured for Reynolds numbers in the range Re_D=8,000~140,000. The results are summarized as follows:

1. The U-groove cylinder was found to reduce the drag coefficient by up to 18.6% compared with the smooth cylinder at $Re_D=1.4\times10^5$, whereas the reduction for the V-groove cylinder was only 2.5%,. The drag reduction of the U-groove cylinder increased with increasing Reynolds number.

2. As the Reynolds number increases, the difference in wake structure with respect to surface configuration increases. The velocity deficit and turbulence intensity in the wake region of the U-groove cylinder is smaller than those for the smooth cylinder.

3. Compared with the smooth and V-groove cylinders, the pressure distributions on the U-groove cylinder show large variations around the separation region of the cylinder. As the Reynolds number increases, the separation point shifted downstream and the surface pressure is decreased. The U-grooves seem to effectively enhance boundary layer transition.

4. The visualized flow past the smooth circular cylinder shows nearly straight pathlines. However, longitudinal secondary vortices are formed near the grooved cylinders. The U-groove cylinder has more active and rapid motion than the smooth cylinder.

Acknowledgements

This work was supported partially by NRL(National Research Laboratory) project and POSTECH.

References

Achenbach, E., 1971, "Influence of Surface Roughness on the Crossflow Around a Circular Cylinder," *J. Fluid Mech.,* Vol. 46, pp. 321~335.

Bearman, P.W., 1969, "On Vortex Shedding from a Circular cylinder in the Critical Reynolds Number Regime," *J. Fluid Mech.*, Vol.37, pp.577~585.

Cantwell, B. J., 1981, "Organized Motion in Turbulent Flow," *Annual Rev. Fluid Mech.*, Vol. 13, pp. 457~515.

Gerrard, J.H., 1954, "A disturbance-sensitive Reynolds Number Range of the Flow Past a Circular Cylinder," *J.Fluid Mech.*, Vol. 22, pp. 187~196.

Guven, O., Farell, C., Patel, V. C., 1980, "Surface Roughness Effects on the Mean Flow Past Circular Cylinders," *J. Fluid Mech.,* Vol. 98, pp. 673~701.

Ko, N.W.M., Leung, Y.C., and Chen, J.J.J., 1986, "Flow Past V-Groove Circular Cylinder," *AIAA Journal*, Vol. 25, No. 6, pp. 806~811.

Leung, Y. C., Ko, N. W. M., 1991, "Near Wall Characteristics of Flow over Grooved Circular Cylinder," *Exp. in Fluids*, Vol. 10, pp. 322~332.

Stansby, P. K., 1974, "The Effect of Endplates on the Base Pressure Coefficient of a Circular Cylinder," *Aeronautical J.*, Vol. 78, pp. 36~37.

Robinson, S. K., 1991, "Coherent Motions in the Turbulent Boundary Layer," *Annual Rev. Fluid Mech.*, Vol. 23, pp. 601~639.

Walsh, M. J., 1983, "Riblets as a Viscous Drag Reduction Technique," *AIAA Journal*, Vol. 21, No. 4, pp. 485~486.